Rational Design of Protein-Based MRI Contrast Agents

Jenny J. Yang,*,[†] Jianhua Yang,[†,‡] Lixia Wei,[‡] Omar Zurkiya,[§] Wei Yang,[†]
Shunyi Li,[†] Jin Zou,[†] Yubin Zhou,[†] Anna L Wilkins Maniccia,[†] Hui Mao,[ll]
Fuqiang Zhao,[§] Russell Malchow,[⊥] Shumin Zhao,[‡] Julian Johnson,[†] Xiaoping Hu,[§]
Eirik Krogstad,[⊥] and Zhi-Ren Liu*,[‡]

*Department of Chemistry, Center for Drug Design and Advanced Biotechnology, Georgia State
University, Atlanta, Georgia 30303, Department of Biology, Georgia State University, Atlanta,
Georgia 30303, Department of Biomedical Engineering, Emory University, Atlanta, Georgia
30333, Department of Radiology, Emory University, Atlanta, Georgia 30333, and Department of
Geosciences, Georgia State University, Atlanta, Georgia 30303*

Received January 29, 2008; E-mail: chejjy@langate.gsu.edu; biozrl@langate.gsu.edu

Abstract: We describe the rational design of a novel class of magnetic resonance imaging (MRI) contrast agents with engineered proteins (CAi.CD2, $i = 1, 2,..., 9$) chelated with gadolinium. The design of protein-based contrast agents involves creating high-coordination Gd^{3+} binding sites in a stable host protein using amino acid residues and water molecules as metal coordinating ligands. Designed proteins show strong selectivity for Gd^{3+} over physiological metal ions such as Ca^{2+}, Zn^{2+}, and Mg^{2+}. These agents exhibit a 20-fold increase in longitudinal and transverse relaxation rate values over the conventional small-molecule contrast agents, e.g., Gd−DTPA (diethylene triamine pentaacetic acid), used clinically. Furthermore, they exhibit much stronger contrast enhancement and much longer blood retention time than Gd−DTPA in mice. With good biocompatibility and potential functionalities, these protein contrast agents may be used as molecular imaging probes to target disease markers, thereby extending applications of MRI.

1. Introduction

Magnetic resonance imaging (MRI) is a noninvasive technique providing high-resolution, three-dimensional images of anatomic structures, as well as functional and physiological information about tissues in vivo. It is capable of detecting abnormalities in deep tissues and allows for whole-body imaging. It has emerged as a primary diagnostic imaging technique.[1,2] Exogenous MRI contrast agents are often used to enhance the contrast between pathological and normal tissues by altering the longitudinal and transverse (i.e., T_1 and T_2) relaxation times of water protons.[3–5] Gadolinium (Gd^{3+}) chelators are the most frequently used MRI contrast agents due to their high magnetic moment, asymmetric electronic ground state, and potential for increased MRI intensity.[6,7] The relaxivity (unit capability of the agent to change the relaxation time) of a contrast agent is dependent on several factors including the number of water molecules in the coordination shell, the exchange rate of the coordinated water with the bulk water, and the rotational correlation time, τ_R, of the molecule.[8–10] It is important for an MRI contrast agent to have (1) high relaxivity for high contrast-to-noise ratio (CNR) and dose efficiency, (2) thermodynamic and chemical stability, especially metal selectivity for the selected lanthanide ions over excess physiological metal ions, to minimize the release of toxic lanthanide ion, (3) adequate vascular, tissue retention time for sufficient imaging time, and (4) propensity for timely excretion from the body.

To date, the most commonly used MRI contrast agent in diagnostic imaging is Gd−DTPA (diethylene triamine pentaacetic acid), or related derivatives such as Gd−DTPA−BMA (bismethylamide). However, with an intrinsic rotational correlation time, τ_R, of 100 ps, these small-molecular Gd^{3+} chelators have longitudinal and transverse proton relaxivities, r_1 and r_2, less than 10 mM^{-1} s^{-1}, much lower than the theoretically maximal value (> 100 mM^{-1} s^{-1}).[9,11] In addition, these small-molecule contrast agents exhibit very short blood circulation (less than 30 min) and tissue retention time, limiting some MRI applications that require longer data collection time.[12] To increase correlation time, τ_R, small-molecular contrast agents

† Department of Chemistry, Center for Drug Design and Advanced Biotechnology, Georgia State University.
‡ Department of Biology, Georgia State University.
§ Department of Biomedical Engineering, Emory University.
ll Department of Radiology, Emory University.
⊥ Department of Geology, Georgia State University.

(1) Tyszka, J. M.; Fraser, S. E.; Jacobs, R. E. *Curr. Opin. Biotechnol.* **2005**, *16* (1), 93–99.
(2) Lippard, S. J. *Nat. Chem. Biol.* **2006**, *2* (10), 504–507.
(3) Louie, A. Y.; Huber, M. M.; Ahrens, E. T.; Rothbacher, U.; Moats, R.; Jacobs, R. E.; Fraser, S. E.; Meade, T. J. *Nat. Biotechnol.* **2000**, *18* (3), 321–325.
(4) Frangioni, J. V. *Nat. Biotechnol.* **2006**, *24* (8), 909–913.
(5) Woods, M.; Woessner, D. E.; Sherry, A. D. *Chem. Soc. Rev.* **2006**, *35* (6), 500–511.
(6) Lauffer, R. B. *Chem. Rev.* **1987**, *87*, 901–927.
(7) Aime, S.; Barge, A.; Cabella, C.; Crich, S. G.; Gianolio, E. *Curr. Pharm. Biotechnol.* **2004**, *5* (6), 509–518.

(8) Toth, E.; Helm, L.; Merbach, A. E. *Top. Curr. Chem.* **2002**, *221*, 61–101.
(9) *The Chemistry of Contrast Agents in Medical Magnetic Resonance Imaging*; Merbach, A. E., Toth, E., Eds.; John Wiley & Sons: Chichester, New York, 2001; p. 471.
(10) Geraldes, C. F.; Sherry, A. D.; Cacheris, W. P.; Kuan, K. T.; Brown, R. D.; Koenig, S. H.; Spiller, M *Magn. Reson. Med.* **1988**, *8* (2), 191–199.
(11) Caravan, P. *Chem. Soc. Rev.* **2006**, *35* (6), 512–523.
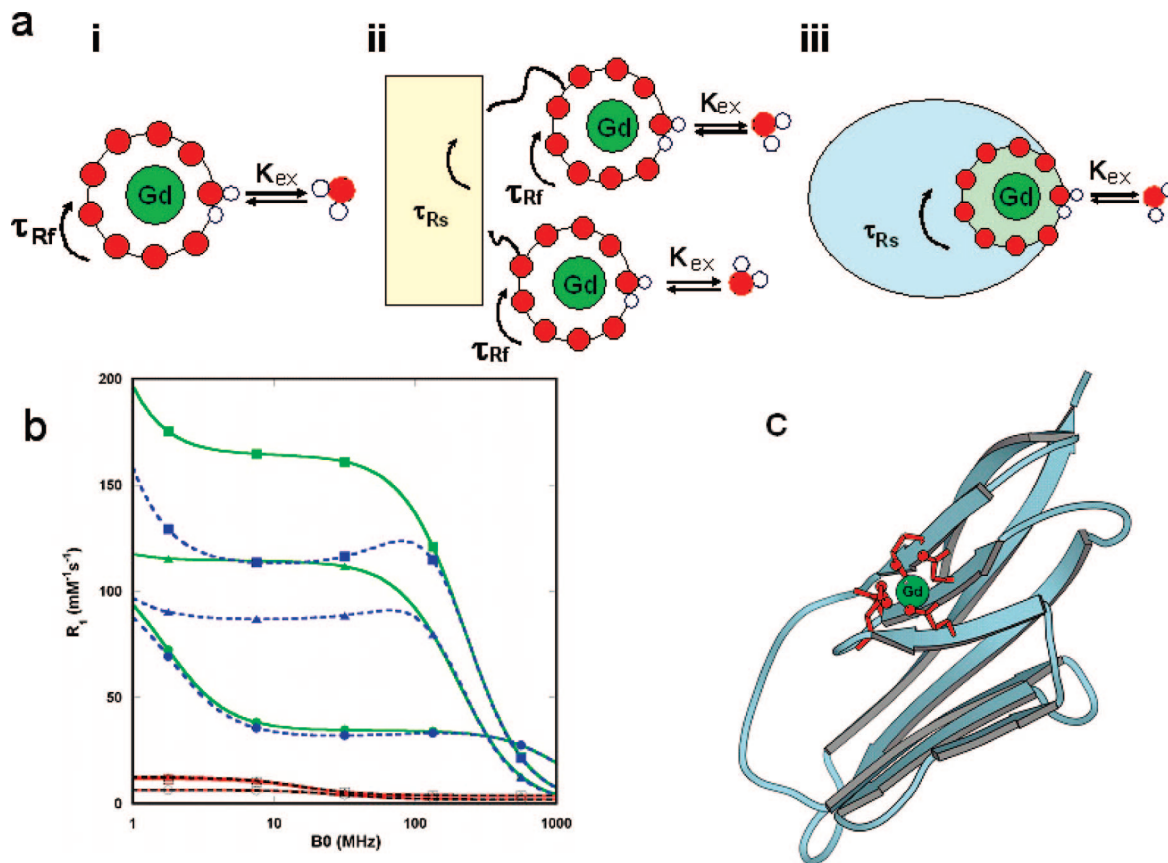
Figure 1. Schematic descriptions of different classes of MRI contrast agents and simulation of T_1 relaxivity. (a) Different constructs of MRI contrast agents. (i) Small chelator DPTA with a fast τ_R (τ_{Rf}) at ~100 ps level; (ii) small contrast agents after being covalently conjugated to macromolecules with a slow τ_R (τ_{Rs}) still possess a fast τ_R due to its internal mobility; (iii) schematic description of the design of reported MRI contrast agents by directly coordinating Gd^{3+} ions to ligand residues on a rigid protein frame to eliminate the high internal mobility. The rotational correlation time of the Gd^{3+} binding site is the same as that of the whole protein (τ_{Rs}). (b) Simulated T_1 relaxivity at the given rotational correlation time τ_R (100 ps, red and black, or 10 ns, green and blue), dwell time τ_m, correlation time of splitting τ_v (1 and 10 ps, solid and dashed lines, respectively), and mean square zero field splitting energy Δ^2 (10^{18} s^{-2}). The τ_m values are 10^{-10} (O), 10^{-9} (□), and 10^{-8} s (△) for 100 ps τ_R and 10^{-9} (●), 10^{-8} (■), and 10^{-7} s (▲) for 10 ns τ_R according to the theory developed by Blombergen and Solomon.[6,7] The water coordination number, q, is assumed to be 1 and the agent concentration is 0.001 M. See Supporting Information for r_1 and r_2 simulations. (c) Modeled structure of designed Gd^{3+}−CA1.CD2 based on the designed NMR structure 1T6W.[28] Ligand residues E15, E56, D58, D62, and D64 at the B, E, and D β-strands of the host protein CD2 are shown in red.

were covalently or noncovalently bound to macromolecules such as linear polymers,[13] dendrimers,[14,15] carbohydrates,[16] proteins,[17–21] viral capsids,[22] and liposomes.[23] An increase in relaxivity was observed when Gd^{3+} binds to calcium binding peptides[24] or proteins such as concanavalin A and bovine serum albumin (BSA).[6] However, the application of these short EF-hand

peptides or proteins as MRI contrast agents is limited due to their weak metal binding affinity for Gd ($K_d \approx 100$ μM for Eu^{3+}) and dynamic flexibility.[24,25] In addition, conjugation yields limited improvement due to internal mobility and restricted water exchange rate (Figure 1a).[11]

Here, we report the development of a new class of MRI contrast agents with significantly improved relaxivity using rational design of Gd^{3+}-binding proteins (CAi.CD2, $i = 1$, 2,..., 9). We chose domain 1 of rat CD2 (referred to as CD2), a cell adhesion protein with a common immunoglobin fold, as a scaffold. CD2 protein exhibits strong stability against pH changes and excellent tolerance against various mutations,[26] which are essential features required for functional protein engineering. In addition, CD2 has a compact structure with

(12) Weinmann, H. J.; Press, W. R.; Gries, H. *Invest. Radiol.* **1990**, *25*, S49–50.

(13) Opsahl, L. R.; Uzgiris, E. E.; Vera, D. R. *Acad. Radiol.* **1995**, *2* (9), 762–767.

(14) Langereis, S.; de Lussanet, Q. G.; van Genderen, M. H.; Meijer, E. W.; Beets-Tan, R. G.; Griffioen, A. W.; van Engelshoven, J. M.; Backes, W. H. *NMR Biomed.* **2006**, *19* (1), 133–141.

(15) Bryant, L. H., Jr.; Brechbiel, M. W.; Wu, C.; Bulte, J. W.; Herynek, V.; Frank, J. A. *J. Magn. Reson. Imaging.* **1999**, *9* (2), 348–352.

(16) Sirlin, C. B.; Vera, D. R.; Corbeil, J. A.; Caballero, M. B.; Buxton, R. B.; Mattrey, R. F. *Acad. Radiol.* **2004**, *11* (12), 1361–1369.

(17) Lanza, G. M.; Winter, P.; Caruthers, S.; Schmeider, A.; Crowder, K.; Morawski, A.; Zhang, H.; Scott, M. J.; Wickline, S. A. *Curr. Pharm. Biotechnol.* **2004**, *5* (6), 495–507.

(18) Karfeld, L. S.; Bull, S. R.; Davis, N. E.; Meade, T. J.; Barron, A. E. *Bioconjug. Chem.* **2007**, *18* (6), 1697–1700.

(19) Gillies, R. J. *J. Cell Biochem. Suppl.* **2002**, *39*, 231–238.

(20) Artemov, D.; Bhujwalla, Z. M.; Bulte, J. W. *Curr. Pharm. Biotechnol.* **2004**, *5* (6), 485–494.

(21) Aime, S.; Cabella, C.; Colombatto, S.; Geninatti Crich, S.; Gianolio, E.; Maggioni, F. *J. Magn. Reson. Imaging* **2002**, *16* (4), 394–406.

(22) Anderson, E. A.; Isaacman, S.; Peabody, D. S.; Wang, E. Y.; Canary, J. W.; Kirshenbaum, K. *Nano Lett.* **2006**, *6* (6), 1160–1164.

(23) Strijkers, G. J.; Mulder, W. J.; van Heeswijk, R. B.; Frederik, P. M.; Bomans, P.; Magusin, P. C.; Nicolay, K. *MAGMA* **2005**, *18* (4), 186–192.

(24) Caravan, P.; Greenwood, J. M.; Welch, J. T.; Franklin, S. J. *Chem. Commun. (Cambridge)* **2003**, (20), 2574–2575.

(25) Kim, Y.; Welch, J. T.; Lindstrom, K. M.; Franklin, S. J. *J. Biol. Inorg. Chem.* **2001**, *6* (2), 173–181.

(26) Wilkins, A. L.; Yang, W.; Yang, J. J. *Curr. Protein Pept. Sci.* **2003**, *4* (5), 367–373.

rotational correlation time, τ_R, of ~10 ns, corresponding to optimal relaxivity for the current clinically allowed magnetic field strength.[27] Moreover, its molecular size (12 kDa) is suitable for good intravascular distribution and easy renal excretion.[17] Our contrast agents were created by designing the metal binding sites into CD2 with desired dynamic properties and metal selectivity to increase relaxivity by optimizing local τ_R. This approach provides a new platform for developing MRI contrast agents with high relaxivity and functionality.

2. Materials and Methods

Determination of the Dynamic Properties of the Designed Proteins. The dynamic properties of the proteins have been monitored via hydrogen exchange and dynamic nuclear magnetic resonance (NMR) using established methods[27,28] and ^{15}N-labeled proteins[29–31] by measuring T_1, T_2, and nuclear Overhauser effect (NOE) to calculate order parameters S^2. Briefly, ^{15}N-enriched protein contrast agents with either 10 mM CaCl$_2$ or 1 mM EGTA used for the backbone dynamic study were engineered, expressed, and purified as previously described.[32] The assignment of NMR spectra of the protein was achieved through standard methods and procedures as previously described.[33] The T_1 and T_2 relaxation times and heteronuclear NOE were measured using conventional pulse sequences.[34,35] The S^2 order parameters were calculated using Modelfree version 4.15 provided by Dr. Palmer of Columbia University.[36,37] The $D_\parallel/D_\perp$ and τ_m were also obtained from the calculation, and the axes of inertia were automatically assigned by the Modelfree program.

Determination of r_1 and r_2 Relaxivity Values. Relaxation times, T_1 and T_2, were determined at 1.5, 3, 9.4 T using Siemens whole-body MR system (1.5, 3 T) or a Bruker MRI scanner (9.4 T). T_1 was determined using inversion recovery and T_2 using a multiecho Carr–Purcell–Meiboom–Gill (CPMG) sequence. The contrast agent samples (200 μL) with different concentrations were placed in Eppendorf tubes. The tubes were placed on a tube rack, which was placed in the MRI scanners for the measurement of relaxation times. r_1 and r_2 were calculated based on r_1 (mM^{-1} s^{-1}) = (1/T_{1s} − 1/T_{1c})/C and r_2 (mM^{-1} s^{-1}) = (1/T_{2s} − 1/T_{2c})/C, where T_{1s} and T_{2s} are relaxation times with contrast agent and T_{1c} and T_{2c} are relaxation times without contrast agent. C is the concentration of contrast agent in mM (the measured Gd^{3+} concentrations by inductively coupled plasma-mass spectrometry (ICP-MS)).

Measurement of Water Coordination Number by Terbium Lifetime Luminescence. The number of water ligands coordinated to the Gd^{3+}−CA1.CD2 complex was determined by measuring Tb^{3+} luminescence decay in H$_2$O or D$_2$O. The Tb^{3+} excited-state lifetime was measured using a fluorescence spectrophotometer (Photon Technology International, Inc.) with a 10 mm path length quartz cell at 22 °C. Following excitation at 265 nm with a XenoFlash lamp (Photon Technology International, Inc.), Tb^{3+} emission was monitored at 545 nm in a time series experiment in both H$_2$O and D$_2$O systems. Luminescence decay lifetime was obtained by fitting the acquired data with a monoexponential decay function. H$_2$O in CA1.CD2 solution was replaced with D$_2$O by lyophilization and redissolved in D$_2$O for at least three times. A standard curve correlating the difference of rate constants obtained in H$_2$O and D$_2$O ($\Delta k_{obs} = k_{H_2O} − k_{D_2O}$) with water number ($q$) under our experimental conditions was established by using well-characterized chelators, such as Tb^{3+}−EDTA ($q = 3$), Tb^{3+}−DTPA ($q = 1$), Tb^{3+}−NTA ($q = 5$), and Aquo Tb^{3+} ($q = 9$) solution with $R^2 = 0.997$.[38,39] The water number coordinated to the Tb^{3+}−CA1.CD2 complex was then obtained by fitting the acquired Δk_{obs} value to the standard curve.

Gd^{3+}-Binding Affinity Determination. Gd^{3+}-binding affinity of CA1.CD2 was determined by a competition titration with Fluo-5N (a metal ion indicator, Invitrogen Molecular Probes) applied as a Gd^{3+} indicator. The fluorescence spectra of Fluo-5N were obtained with a fluorescence spectrophotometer (Photon Technology International, Inc.) with a 10 mm path length quartz cell at 22 °C. Fluo-5N emission spectra were acquired at 500−650 nm with an excitation at 488 nm. Gd^{3+}-binding affinity of Fluo-5N, K_{d1}, was first determined by a Gd^{3+} titration with Gd^{3+} buffer system of 1 mM nitrilotriacetic acid (NTA). Free Gd^{3+} concentration was calculated with a NTA Gd^{3+}-binding affinity of 2.6×10^{-12} M.[40] Fluo-5N was mixed with Gd^{3+} in 1:1 ratio for a competition titration. The experiment was performed with a gradual addition of CA1.CD2. An apparent dissociation constant, K_{app}, was estimated by fitting the fluorescence emission intensity of Fluo-5N at 520 nm with different CA1.CD2 concentrations as a 1:1 binding model. Gd^{3+}-binding affinity of CA1.CD2, K_{d2}, was calculated with the following equation:

$$K_{d2} = K_{app} \frac{K_{d1}}{K_{d1} + [\text{Fluo} - 5N]_T} \tag{1}$$

Mouse MR Imaging. CD-1 mice (25−30 g, $N = 4$) were used for MRI experiments. Care of experimental animals was conducted in accordance with institutional guidelines. Each animal was anesthetized with an isoflurane gas mixture and then positioned and stabilized in the scanner in the coil cradle. Each animal was kept warm during the MRI scan. The mice were scanned before and after the administration of any contrast agents. For contrast-enhanced MRI, ~50 μL of Gd^{3+}−CA1.CD2 (~1.2 mM) or Gd^{3+}−DTPA (~300 mM) were injected into the animal via the tail vein. MR images were collected at multiple times. For T_1-weighted imaging at 3 T, spin echo sequence with TE/TR = 15 ms/500 ms was employed. Rectangular field of view (FOV) at 100/40 mm, an acquisition matrix of 196^2 and 1.1 mm slice thickness without gap were used. Images were collected from both transverse and coronal sections. The in-plane resolution of images was less than 0.5 mm after they were reconstructed to the matrix of 196.^{2} For T_2-weighted imaging at 9.4 T, MR images were recorded using a multiecho CPMG sequence. The data were collected and analyzed using Dicomworks software. The MR signal intensity in several organs was ascertained by the average intensity in the defined regions of interest (ROIs) or voxels within the organs. Signal intensity for each organ was normalized to that of the leg muscle.

(27) Yang, W.; Wilkins, A. L.; Li, S.; Ye, Y.; Yang, J. J. *Biochemistry* **2005**, *44* (23), 8267–8273.

(28) Yang, W.; Wilkins, A. L.; Ye, Y.; Liu, Z. R.; Li, S. Y.; Urbauer, J. L.; Hellinga, H. W.; Kearney, A.; van der Merwe, P. A.; Yang, J. J. *J. Am. Chem. Soc.* **2005**, *127* (7), 2085–2093.

(29) Farrow, N. A.; Muhandiram, R.; Singer, A. U.; Pascal, S. M.; Kay, C. M.; Gish, G.; Shoelson, S. E.; Pawson, T.; Forman-Kay, J. D.; Kay, L. E. *Biochemistry* **1994**, *33* (19), 5984–6003.

(30) Barbato, G.; Ikura, M.; Kay, L. E.; Pastor, R. W.; Bax, A. *Biochemistry* **1992**, *31* (23), 5269–5278.

(31) Nicholson, L. K.; Kay, L. E.; Baldisseri, D. M.; Arango, J.; Young, P. E.; Bax, A.; Torchia, D. A. *Biochemistry* **1992**, *31* (23), 5253–5263.

(32) Yang, W.; Jones, L. M.; Isley, L.; Ye, Y.; Lee, H. W.; Wilkins, A.; Liu, Z. R.; Hellinga, H. W.; Malchow, R.; Ghazi, M.; Yang, J. J. *J. Am. Chem. Soc.* **2003**, *125* (20), 6165–6171.

(33) Akke, M.; Skelton, N. J.; Kordel, J.; Palmer, A. G.; Chazin, W. J. *Biochemistry* **1993**, *32* (37), 9832–9844.

(34) Kay, L. E.; Keifer, P.; Saarinen, T. *J. Am. Chem. Soc.* **1992**, *114*, 10663–10665.

(35) Bendall, M. R. *J. Magn. Reson., Ser. A* **1995**, *116*, 46–58.

(36) Palmer, A. G.; Rance, M.; Wright, P. E *J. Am. Chem. Soc.* **1991**, *113*, 4371–4380.

(37) Palmer, A. G. *Annu. Rev. Biophys. Biomol. Struct.* **2001**, *30*, 129–155.

(38) Sudnick, D. R.; Horrocks, W. D., Jr. *Biochim. Biophys. Acta* **1979**, *578* (1), 135–144.

(39) Beeby, A.; Clarkson, I. M.; Dickins, R. S.; Faulkner, S.; Parker, D.; Royle, L.; de Sousa, A. S.; Gareth Williams, J. A.; Woods, M. *J. Chem. Soc., Perkin Trans.* **1999**, *2*, 493–504.

(40) Martell, A. E.; Simth, R. M.; Motekaitis, R. J., *NIST Standard Reference Data*, Gaithersburg, MD 1993.

Blood Circulation Time, Tissue Retention Time, and Biodistribution. Appropriate dosages of Gd^{3+}–CA1.CD2 or Gd^{3+}–DTPA were intravenously (i.v.) injected (via tail vein). Blood ($\sim$50 μL) samples were collected via orbital sinus at different time points. Each of the animals ($N = 4$) was euthanized at the final time point. Tissue samples from kidney, liver, heart, and lung were collected. Serum samples were prepared from the collected blood. For the biodistribution analyses, the animals were euthanized at a single time point (indicated) after i.v. administration of the contrast agent (indicated). The organ/tissue samples were collected. Tissue extracts were freshly made from collected samples using commercially available tissue extracting kits (Qiagen). CA1.CD2 was detected and quantified by immunoblotting and sandwich enzyme-linked immunosorbent assay (Sandwich-ELISA) using a monoclonal antibody (OX45, detecting antibody) and a homemade polyclonal antibody (PabCD2, capture antibody). A series of known amounts of CA1.CD2 samples mixed with blank mouse serum or tissue extracts were used as standard in Sandwich-ELISA. ELISA signal from Horseradish peroxidase (HRP) was monitored using a Fluostar fluorescence microplate reader. For quantification of Gd^{3+} in the serum and tissue samples 1 h (or indicated times) after the contrast agent administration, animals were sacrificed and critical organs were collected, and the tissues were then digested with concentrated nitric acid at 120–130 °C with proper amount of ^{157}Gd spike as an internal marker. The digested solution was analyzed by ICP-MS (Element 2) using an isotope dilution method.

Toxicity Analyses. After MRI experiments, CD-1 mice that received Gd^{3+}–CA1.CD2 (at a dose of $\sim$2.4 μmol/kg) were returned to their cages (one mouse per cage). The mice were observed for 5 days and were euthanized at the end of the fifth day. Tissue samples from kidney, liver, spleen, and lung were collected. Gd^{3+} ion contents in the tissue samples were analyzed by ICP-MS (see above paragraph).

Two groups of mice were used to examine potential renal and/ or liver damage by Gd^{3+}–CA1.CD2. One group of mice received (i.v. tail veil) 50 μL of saline buffer as control. Another group received (i.v. tail veil) Gd^{3+}–CA1.CD2 at a dosage of 4 μmol/kg. The mice were observed for 48 h and were euthanized. Blood samples were collected from the experimental mice. Serum samples were prepared from the collected blood. Liver enzymes in serum samples, including Alanine transaminase (ALT), Alkaline phosphatase (ALP), Aspartate transaminase (AST), Gamma glutamyl transpeptidase (GGT), and bilirubin and urea nitrogen were analyzed by a commercially available source (MU Research Animal Diagnostic Laboratory). All histo-chemistry parameters were measured on an Olympus AU 400 analyzer.

Cytotoxicity was analyzed by MTT (3-(4,5-dimethylthiazol-2-yl)-2,5-diphenyltetrazolium bromide) assay of the cells that were treated with Gd–CA1.CD2 at appropriate doses (indicated in Supporting Information, Figure S4b). The cells were grown under normal growth medium in 96 well plates. Gd–CA1.CD2 or saline-phosphate buffer was added to the cell culture medium. The cells were incubated for appropriate times. A standard MTT assay was employed to assess the cell growth status of the treated cells.

Serum Stability. CA1.CD2 (40 μM) in complex with Gd^{3+} was incubated with 75% human serum over 3 or 6 h at 37 °C. The degradation of the protein (disappearance of 12 kDa protein band) was analyzed by sodium dodecyl sulfate polyacrylamide gel electrophoresis (SDS-PAGE) and visualized by coomassie blue staining. In parallel, the degradation of the protein was also analyzed by immunoblotting using antibodies OX54 or PabCD2. The identities of the 12 kDa bands as CA1.CD2 were always verified by immunoblotting using antibody PabCD2.

3. Results

Rational Design of Gd^{3+}-Binding Proteins. Figure 1 shows the simulation of the dependence of r_1 and r_2 on the rotational correlation time, τ_R, of a contrast agent at different magnetic

field strengths according to the theory developed by Blombergen and Solomon[6,7] (for detailed simulation procedures, please see online Supporting Information). For small molecules such as Gd^{3+}–DPTA with τ_R at hundreds of ps, the relaxivity is <10 mM^{-1} s^{-1} regardless of how the other parameters are adjusted. On the other hand, the simulation clearly suggests that contrast agents with τ_R of 10–50 ns have the highest r_1 and r_2 values at clinically relevant magnetic field strengths from 0.47–4.7 T.[11] Thus, we envisioned that high-relaxivity MRI contrast agents can be developed by directly designing Gd^{3+} binding sites in proteins with desired τ_R. Coordinating Gd^{3+} ions directly to the rigid protein frame eliminates the high internal mobility associated with chelator-macromolecule conjugates (Figure 1a).

We next designed a series of Gd^{3+} binding sites into CD2 using computational methods.[41,42] These designs were based on established structural parameters obtained from detailed analysis of metal binding sites in over 500 small chelators and metalloproteins. Gd^{3+}, Tb^{3+}, La^{3+}, and other Ln^{3+} ions have coordination properties similar to those of Ca^{2+} with a strong preference for oxygen ligand atoms.[43] Small chelators usually have an average 9.3 and 6.9 total coordinating atoms for Gd^{3+} and Ca^{2+}, respectively. For example, DTPA has five oxygen ligand atoms and two nitrogen ligand atoms. For macromolecules such as proteins, the coordination atoms are almost always oxygen atoms and the coordination numbers are lower than small chelators with an average of 7.2 for Ln^{3+} and 6.0–6.5 for Ca^{2+}. These effects are possibly due to steric crowding and side chain packing.[43] Previously, we successfully designed Ca^{2+} and Ln^{3+} binding sites in a scaffold protein with strong target metal selectivity in the presence of excess physiological metal ions.[32] Structure determination by solution NMR revealed that the actual coordination geometry in a designed variant is the same as our design, verifying the computational methods and the design strategy of metal-binding sites in proteins.[28]

The designed proteins were named as CAi.CD2, $i = 1, 2,..., 9$, reflecting Gd^{3+}-binding sites at different locations. Figure 1c shows an example of designed Gd^{3+}-binding protein CA1.CD2 with a metal binding site formed by the six potential oxygen ligands from the carboxyl side chains of Glu15, Glu56, Asp58, Asp62, and Asp64. On the basis of our studies of charged residues in the coordination shell,[44] we placed five negatively charged residues in the coordination shell of CA1.CD2 to provide six oxygen ligand atoms to increase the selectivity for Gd^{3+} over Ca^{2+}. To achieve the desired relaxation property, one position of the metal binding geometry was left open in the design to allow fast water exchange between the paramagnetic metal ion and the bulk solvent (Figure 1a). Importantly, the Gd^{3+}-binding site has minimal internal flexibility as the ligand residues originate from rigid stretches of the protein frame. To test the requirement for rigid embodiment in achieving high relaxivity, another Gd^{3+}-binding protein, CA9.CD2, was engineered by fusing a continuous cation-binding EF-hand loop from calmodulin (CaM) with flexible glycine linkers to the host protein.[45,46] The properties of this protein mimic previously reported, highly flexible chelate-based contrast agents conjugated to macromolecules.[24,25]

(41) Deng, H.; Chen, G.; Yang, W.; Yang, J. J. *Proteins* **2006**, *64* (1), 34–42.

(42) Yang, W.; Lee, H. W.; Hellinga, H.; Yang, J. J. *Proteins* **2002**, *47* (3), 344–356.

(43) Pidcock, E.; Moore, G. R. *J. Biol. Inorg. Chem.* **2001**, *6* (5–6), 479–489.

(44) Maniccia, A. W.; Yang, W.; Li, S. Y.; Johnson, J. A.; Yang, J. J. *Biochemistry* **2006**, *45* (18), 5848–5856.

Table 1. Metal Binding Constants (log K_a) and Metal Selectivity of DTPA, DTPA-BMA, and CA1.CD2

sample	Gd^{3+}	Zn^{2+}	Ca^{2+}	Mg^{2+}	log (K_{Gd}/K_{Zn})	log (K_{Gd}/K_{Ca})	log (K_{Gd}/K_{Mg})
DTPA[40]	22.45	18.29	10.75	18.20	4.17	11.70	4.25
DTPA-BMA[49]	16.85	12.04	7.17	na[a]	4.81	9.68	na[a]
CA1.CD2	12.06	6.72	<2.22	<2.0	5.34	>9.84	>10.06

^{a} na: not available.
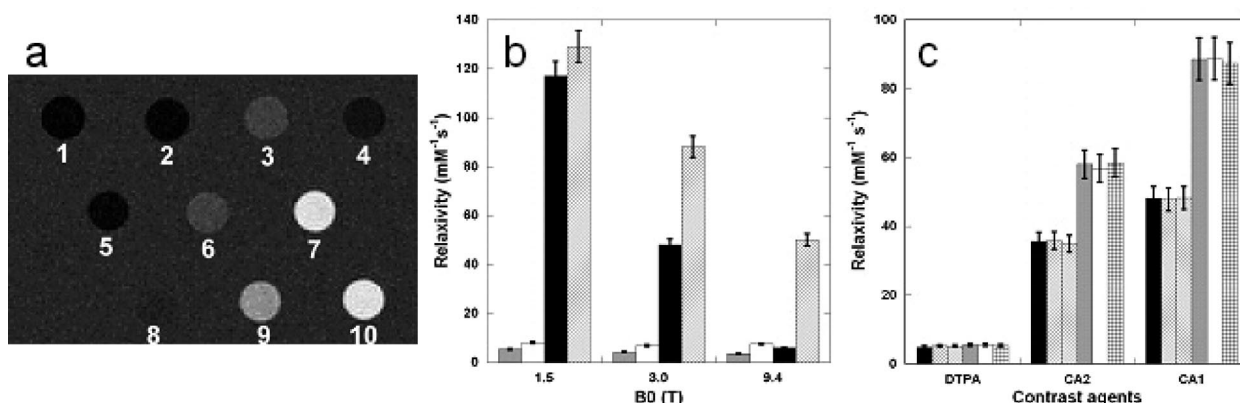
Figure 2. Comparison of in vitro relaxivity between Gd^{3+}-DTPA and designed contrast agents. (a) MR images produced using an inversion recovery sequence (TR 6000 ms, TI 960 ms, and TE 7.6 ms) at 3 T. Samples are (1) dH$_2$O, (2) 10 mM Tris-HCl pH 7.4, (3) 0.10 mM Gd^{3+}−DTPA in H$_2$O, (4) 0.10 mM Gd^{3+}−DTPA in 10 mM Tris-HCl pH 7.4, (5) 0.10 mM GdCl$_3$ and CD2, 6) 0.077 mM Gd^{3+}−CA4.CD2, (7) 0.050 mM Gd^{3+}−CA2.CD2, (8) 0.10 mM Gd^{3+}−CA9.CD2, (9) 0.020 mM Gd^{3+}−CA1.CD2, and (10) 0.050 mM Gd^{3+}−CA1.CD2. (b) Proton relaxivity values of Gd^{3+}−CA1.CD2 (r_1, solid black; r_2, cross) and Gd^{3+}−DPTA (r_1, shield; r_2, open) at indicated field strength were measured as a function of field strength. (c) In vitro relaxivity of contrast agents Gd^{3+}−DPTA (DTPA), Gd^{3+}−CA1.CD2 (CA1), and Gd^{3+}−CA2.CD2 (CA2) in the absence of Ca^{2+} (black and gray), presence of 1 mM Ca^{2+} (left strip and open) and 10 mM Ca^{2+} (right strip and cross) at 3 T. T_1 (black, left and right strips) and T_2 (gray, open and cross) were determined using a Siemens whole-body MR system.

All of the designed Gd^{3+} binding proteins were expressed in *Escherichia coli* and subsequently purified by procedures previously published from our laboratory.[27,28] All of the designed proteins form the expected metal-protein complex as demonstrated by electrospray ionization-mass spectrometry (ESI-MS) (Supporting Information, Figure S1). Since metal selectivity for Gd^{3+} over other physiological metal ions is important for minimizing the toxicity of the agents,[47,48] we measured metal binding constants using dye-competition assays with various chelate−metal buffer systems (Table 1, Supporting Information, Figure S2). Low-limit metal binding affinities of the proteins were also estimated based on Tb^{3+}-sensitized fluorescence resonance energy transfer (FRET) and competition assays. CA1.CD2 exhibited disassociation constants (K_d, M) of 7.0×10^{-13}, 1.9×10^{-7}, 6×10^{-3}, and $>1 \times 10^{-2}$ for Gd^{3+}, Zn^{2+}, Ca^{2+}, and Mg^{2+}, respectively. The selectivity K_d^{ML}/K_d^{GdL} for Gd^{3+} over physiological divalent cations Zn^{2+}, Ca^{2+}, and Mg^{2+} are $10^{5.34}$, $>10^{9.84}$, and $>10^{10.06}$, respectively. The Gd^{3+} selectivity of CA1.CD2 is significantly greater than or comparable to that of the Food and Drug Administration (FDA) approved contrast agents DTPA- and DTPA-BMA[48] (Table 1). The high Gd^{3+} binding selectivity of CA1.CD2 was further supported by the observation that r_1 and r_2 of Gd^{3+}−CA1.CD2 were not altered in the presence of excess Ca^{2+} (10 mM) (Figure 2). Further assays showed that potential chelators in serum, such

as phosphate (50 mM), were not able to remove the Gd^{3+} from the Gd^{3+}−protein complex. This is important for in vivo applications of the contrast agent as the phosphate concentration in serum is maintained at ~1.3 mM.[6,9] The stability of a contrast agent in blood circulation is another important factor for in vivo applications. We characterized the stability by incubating Gd^{3+}−CA1.CD2 with 75% human serum at 37 °C for 3 and 6 h. The Gd^{3+}−protein complex remained intact after 6 h of incubation, indicating that the Gd^{3+}−protein complex is stable in blood. Taken together, the designed Gd^{3+}−protein contrast agent is comparable to the clinically used contrast agents in Gd^{3+} binding stability and selectivity.[6,7]

Designed Gd^{3+}-Binding Proteins Exhibit High r_1 and r_2 Relaxivity. We have determined the relaxivity values of the designed protein contrast agents at field strengths of 1.5, 3.0, and 9.4 T field strengths (Figure 2). Figure 2a shows that, at a concentration of 50 μM, the designed contrast agents Gd^{3+}−CA1.CD2 and Gd^{3+}−CA2.CD2 were able to introduce contrast enhancement in T_1-weighted imaging at 3.0 T while 100 μM Gd^{3+}−DTPA and protein CA1.CD2 alone did not lead to significant enhancement. The in vitro relaxivity values of the designed Gd^{3+}-binding proteins were measured (Table 2). Gd^{3+}−CA1.CD2 exhibits r_1 up to 117 mM^{-1} s^{-1} at 1.5 T, about 20-fold higher than that of Gd^{3+}−DTPA. In contrast, Gd^{3+}−CA9.CD2, which carries a flexibly conjugated Gd^{3+}-binding site, had significantly lower relaxivity values (3.4 and 3.6 mM^{-1} s^{-1}, for r_1 and r_2, respectively, at 3.0 T), that are comparable to those of Gd^{3+}−DTPA (Table 2). These data support the conjecture that elimination of the intrinsic mobility of the metal binding site resulted in the desired high relaxivity values.

(45) Ye, Y.; Lee, H. W.; Yang, W.; Shealy, S. J.; Wilkins, A. L.; Liu, Z. R.; Torshin, I.; Harrison, R.; Wohlhueter, R.; Yang, J. J. *Protein Eng.* **2001**, *14* (12), 1001–1013.

(46) Ye, Y.; Lee, H. W.; Yang, W.; Shealy, S.; Yang, J. J. *J. Am. Chem. Soc.* **2005**, *127* (11), 3743–3750.
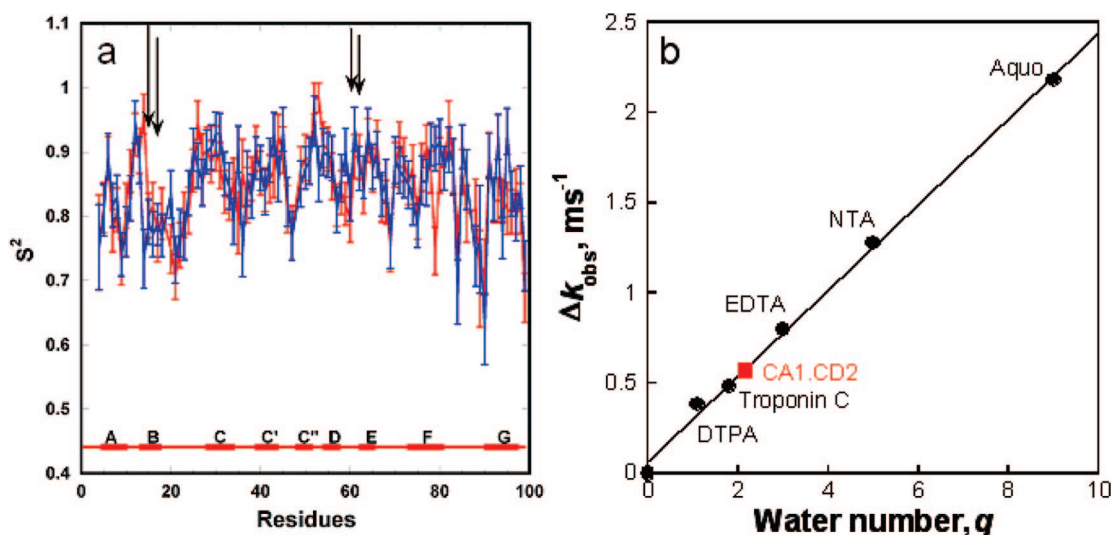
(47) Wedeking, P.; Shukla, R.; Kouch, Y. T.; Nunn, A. D.; Tweedle, M. F. *Magn. Reson. Imaging* **1999**, *17* (4), 569–575.

(48) Kumar, K.; Tweedle, M. F.; Malley, M. F.; Cougoutas, J. Z. *Inorg. Chem.* **1995**, *34*, 6472–6480.

(49) Cacheris, W. P.; Quay, S. C.; Rocklage, S. M. *Magn. Reson. Imaging* **1990**, *8* (4), 467–481.

Table 2. Proton Relaxivity of Different Classes of Contrast Agents

CA class	compounds (ligand residues)	r_1 (mM^{-1} s^{-1})	r_2 (mM^{-1} s^{-1})	B0 (T)	MW (kDa)
designed proteins	Gd^{3+}−CA1.CD2	117	129	1.5	12
	(E15/E56/D58/D62/D64)	48	88	3	
		6	50	9.4	
	Gd^{3+}−CA2.CD2 (D15/D17/N60/D62)	35	58	3	12
	Gd^{3+}−CA3.CD2	130		1.5	
	(E15/E56/D58/D62/E64)	34	57	3	12
	Gd^{3+}−CA9.CD2 (add EF-loop III from Calmodulin)	3.5	3.6	3	12
small compound	Gd^{3+}−DTPA	5.4	8	1.5	0.743
		4.2	6.8	3	
protein carriers[a]	albumin	11.5	12.4	0.25	80
	poly(lysine)	13	15	0.47	52
dendrimers[a]	gadomer-17	13		1.5	35
liposome[a]	ACPL	12	11	1.5	>10^3
nanoparticle emulsion[a]	Gd^{3+}-perfluorocarbon nanoparticles	34	50	1.5	>10^3

[a] Based on refs 17, 19–21.

Figure 3. Dynamic properties and hydration water number of designed contrast agents. (a) S^2 order values of the engineered metal binding protein. The positions of ligand residues are shown in vertical bars. Order parameters of CA1−CD2 with discontinuous ligand residues have the same dynamic properties as the scaffold protein. Arrows indicate the position of ligand residues. (b) Measurement of coordination water number by monitoring the Tb^{3+} lifetime. The luminescence decay lifetime was obtained by fitting the acquired data in both H$_2$O and D$_2$O with a monoexponential decay function. A standard curve correlating the Δk_{obs} with water number (q) was established by using well-characterized chelators, such as EDTA ($q = 3$), DTPA ($q = 1$), NTA ($q = 5$), and Aquo Tb^{3+} ($q = 9$) solution with $R^2 = 0.997$.[38,39] Water numbers coordinated to Tb^{3+}−protein complexes were then obtained by fitting the acquired Δk_{obs} value to the standard curve.

The r_1 and r_2 of Gd^{3+}−CA1.CD2 exhibited an inverse relationship with the magnetic field strength (Table 2). In contrast, the r_1 and r_2 of Gd^{3+}−DPTA showed weak dependence on field strengths. The magnetic field strength dependent changes in relaxivity are consistent with our simulation results based on the rotational τ_R of the contrast agent (Figure 1b). The results showed that the protein contrast agent offers much higher relaxivities for MRI contrast enhancement at clinical magnetic field strengths (1.5−3.0 T). Interestingly, the transverse relaxivity of the designed contrast agent is very high (e.g. >50 mM^{-1} s^{-1}) at 9.4 T compared to Gd^{3+}−DTPA, making it appropriate as a T_2 contrast agent (Table 2) at high fields. It should be pointed out that r_2 of our protein-based contrast agent is smaller than the currently used r_2 agents such as iron oxides.[50] This property allows our contrast agents to fill an important gap between small Gd chelators and iron oxide nanoparticles, extending the range of MRI applications both at clinically relevant field strength and possibly higher field strength.

One key factor that contributes greatly to the relaxivity of an MRI contrast agent is its rotational correlation time, τ_R.[11,27,28] Dynamic NMR studies showed that the overall correlation time of our designed protein (CA1.CD2) is similar in the absence (9.20 ns) and presence of bound metal ions (9.08 ns), consistent with that for proteins of similar size.[51] The values of the order parameter S^2 of the ligand residues are similar to the average value of the protein, suggesting that the metal binding pocket tumbles with the protein as a whole (Figure 3a). Therefore, the measured correlation time of the protein directly reflects the τ_R of the metal binding site. In contrast, the flexible metal binding loop in CA9.CD2 has an S^2 order value of 0.3−0.4 (unpublished data), which is very different from CA1.CD2 with an S^2 value very close to that of the backbone of the protein.

The hydration number of an MRI contrast agent is another important determinant for r_1 and r_2. The hydration number of the designed protein-based contrast agents was determined by measuring the luminescence lifetime of Tb^{3+}.[38] The free Tb^{3+}

(50) Bulte, J. W.; Kraitchman, D. L. *NMR Biomed.* **2004**, *17* (7), 484–499.

(51) Wyss, D. F.; Dayie, K. T.; Wagner, G. *Protein Sci.* **1997**, *6* (3), 534–542.
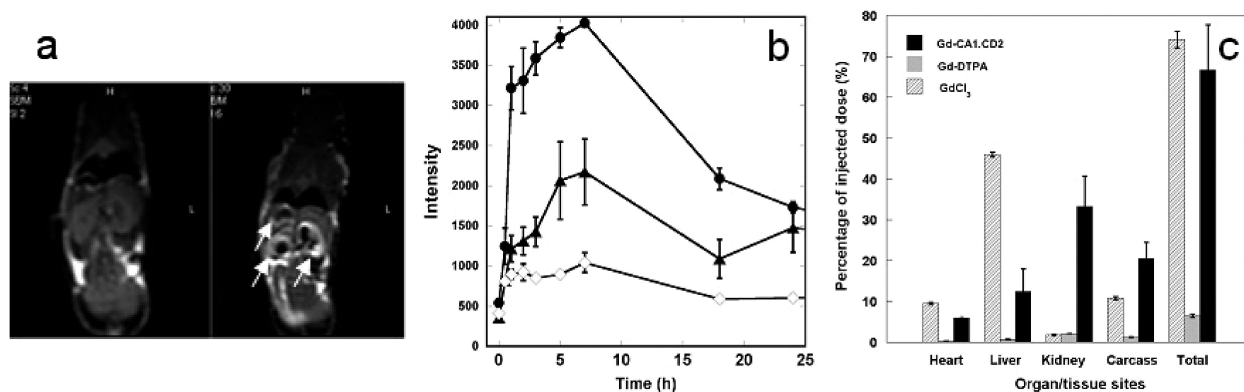
Figure 4. In vivo MR images and biodistribution of designed contrast agents. (a) MR images of mouse (26 g) pre (left) and 40 min post (right) injection of 50 μL of 1.2 mM Gd^{3+}−CA1.CD2 through the tail vein. The MRI was performed using a spin echo sequence with TE/TR = 15 ms/500 ms using a 3 T scanner. The arrows indicate the contrast enhancements at different organ sites. (b) The MRI signal intensity changes at kidney (•), liver (▲), and muscle (◇) as a function of time. The 0 refers to the preinjection. (c) Tissue distributions 1 h postintravenous injection of Gd^{3+}−CA1.CD2 (3.0 μmol/kg, solid black), Gd^{3+}−DTPA (150 μmol/kg, gray), and $GdCl_3$ (100 μmol/kg, open). The Gd^{3+} in tissues was measured by ICP-MS and was calculated and expressed as a percentage of the injected dose.[53] The Gd^{3+} retained in the animal carcass (i.e., the remainder of the whole body after removing indicated organs) is calculated as the mean from 10 randomly selected sites. Error bars in (a), (b), and (c) are standard deviations of four measurements or four animals (n = 4).

in H_2O and D_2O has lifetime values of 410 and 2796 μs, respectively. The formation of the Tb^{3+}−protein complex in H_2O significantly increases Tb^{3+} lifetime to 859 μs. The Tb^{3+} lifetime value of CA1.CD2 was 1679 μs in D_2O, suggesting a hydration number of 2.1 (Figure 3b). Interestingly, a well-known Ca^{2+}-binding protein troponin C exhibits a hydration number of 1.8 (Figure 3b). It was determined by the X-ray crystal structure that troponin C has only one water molecule coordinated Tb^{3+} in the metal binding pocket.[52] The effect of second and outer-sphere oscillators on hydration number is further indicated with a revised equation[39] in which the effect of second and outer-sphere oscillators on hydration number results in increased hydrogen numbers 2.5 and 3.0 for troponin C and CA1.CD2, respectively. Therefore, it is conceivable that the hydration water molecules either from the coordination shell or the outer shell of the protein also contribute to the observed high relaxivity of CA1.CD2.

Contrast-Enhanced MR Imaging of Mice. The effect of MRI contrast enhancement of the protein contrast agent was tested in mice (CD-1 mice). Gd^{3+}−CA1.CD2 was administered via tail vein at a dose of ∼2.4 μmol Gd^{3+}/kg of body weight, about 35-fold lower than the dosage of Gd^{3+}−DTPA used in diagnostic imaging. Comparison of pre- and postcontrast T_1 weighted spin echo images obtained at 3 T showed the contrast enhancement in several organs with the greatest enhancement of the MRI contrast observed in the kidney (Figure 4a, arrows indicated), which exhibited a time dependent change of the contrast enhancement over a period of 24 h (Figure 4b). Quantitative analysis of image data showed the distribution of the contrast enhancement at different organs (Figure 4b). The tissue-dependent enhancement is consistent with the biodistribution of Gd^{3+} analyzed at 1 h time point using ICP-MS (Figure 4c). The T_1 contrast enhancement in the kidney cortex diminished substantially at 18 h after the administration of Gd^{3+}−CA1.CD2, suggesting that the agent was gradually cleared from the kidney and other organs. Consistent with the simulations and relaxivity values determined in vitro, a strong T_2 contrast enhancement was observed at 9.4 T. T_2-weighted

images at 9.4 T, and T_1-weighted images at 3 T showed very similar tissue and organ distribution patterns (Supporting Information, Figure S3). Conversely, Gd^{3+}−DTPA at the same concentration failed to exhibit contrast enhancements at either 3 or 9.4 T.

Furthermore, contrast enhancement by Gd^{3+}−CA1.CD2 was sustained over 4−7 h at multiple organs (Figure 4b), indicating much longer tissue retention time of Gd^{3+}−CA1.CD2 than that of Gd^{3+}−DTPA. The tissue retention and blood circulation times of Gd^{3+}−CA1.CD2 in mice were characterized by administering various doses of agents in mice and analyzing the collected blood samples or tissue sections from sacrificed animals using immunoblots and ELISA with monoclonal (OX45) and in-house-developed polyclonal (PabCD2) antibodies. In contrast to the short blood circulation time of Gd^{3+}−DPTA, Gd^{3+}−CA1.CD2 exhibited a prolonged blood circulation time. No significant decrease in the CA1.CD2 levels in blood was observed until 45 min after i.v. administration. The protein remained in blood circulation for more than 3 h (Supporting Information, Figure S4a). This property is important for imaging of biological events that require prolonged imaging time, or imaging of pathological features that require time for delivery of the agent to the targeted site. In the kidney, CA1.CD2 was first detectable at 15 min and peaked at 4−5 h. There was less than 10% of the injected dose of the contrast agent remaining in the kidney 15 h after injection (by measurements of both Gd^{3+} and CA1.CD2). This result, along with the observation of MRI contrast changes in the bladder, suggests a clearance of the agent by kidney.

Gd^{3+}−CA1.CD2 did not exhibit acute toxicity at the dose (∼2.4 μmol/kg) used for MRI. All mice that received the contrast agents (>10 times) showed no adverse effects before euthanization five days after agent injection. The effects of Gd^{3+}−CA1.CD2 on liver enzymes (ALT, ALP, AST), serum urea nitrogen, bilirubin, and total protein from CD-1 mice 48 h postcontrast injection were negligible compared to those in the control mice (Table S1). In addition, no cytotoxicity was observed in tested cell lines, SW620, SW480 and HEK293 that

(52) Rao, S. T.; Satyshur, K. A.; Greaser, M. L.; Sundaralingam, M. *Acta Crystallogr. D: Biol. Crystallogr.* **1996**, *52* (Pt 5), 916–922.

(53) Barnhart, J. L.; Kuhnert, N.; Bakan, D. A.; Berk, R. N. *Magn. Reson. Imaging* **1987**, *5* (3), 221–231.

were treated with 50 μM Gd^{3+}−CA1.CD2, by MTT assay (Supporting Information, Figure S4b). On the basis of the preliminary characterization of toxicity, we conclude that the protein contrast agent did not exhibit acute toxicity at current dosages for mice.

4. Discussion

While new developments of Gd^{3+} chelators[4,5,11,21,54] continue to expand the applications of small-molecular contrast agents, macromolecular agents are increasingly attractive for functional and molecular imaging applications. A common approach of using small-molecular Gd^{3+}−DTPA to bind albumin in serum (e.g., MS-325) has the capability to enhance the relaxivity *in vivo*. However, this class of contrast agents is currently limited to imaging the vascular system[55–58] with its complex pharma-cokinetics.[59] Conjugation or encapsulation of small Gd^{3+} chelators to or in liposome, fullerene and nanotubes indeed resulted in increases in relaxivity; however, several important drawbacks limit the applications of these agents. Our approach of using an engineered protein to chelate the Gd^{3+} for contrast enhancing effects differs fundamentally from those previous studies in several respects. First, we have created a Gd^{3+}-binding site with strong metal selectivity in a stable and potentially fully functioning host protein by de novo design. This is significantly different from using a small peptide fragment to cross-link a small Gd^{3+} chelate for enhanced stability and rigidity of the binding site, as well as biological function of the biomolecule matrix. To our knowledge, this is the first example where a protein-based MRI contrast agent was developed using an engineered Gd^{3+}-binding protein without using existing small metal chelators. This is an important achievement in protein design, involving the rational development of a metalloprotein with high coordination number and charged ligand residues in the coordination shell. Second, our approach provides a new platform for developing by protein engineering high-performance MRI contrast agents with further improved relaxivity and metal selectivity and stability. Our studies reveal that three factors are key in achieving high relaxivity: (1) longer rotational correlation time τ_R of the designed agents, (2) direct coordination of Gd^{3+} ions to amino acid ligands from the rigid protein matrix to eliminate internal mobility, and (3) increased number of hydration water molecules. As predicted by the Solomon−Bloembergen−Morgan equation (Supporting Information, eq 1), relaxivities can be significantly increased by increasing the number of hydration water molecules. Unfortunately, previous attempts to increase relaxivities by increasing the number of coordinating water molecules >1 for BTPA and DTPA−BMA

did not yield expected results. Our studies demonstrated that it is possible to increase relaxivity by increasing the hydration number of a protein MRI contrast agent without sacrificing metal binding properties, such as affinity and metal specificity. Although the Gd/Zn selectivity for our developed CA1.CD2 is better than for Gd^{3+}−DTPA−BMA, as shown in Table 1, further improvement in the kinetic stability and metal selectivity may be necessary to prevent the risk of clinical problems such as Nephrogenic systemic fibrosis (NSF) related to the kinetically controlled *in vivo* release of Gd^{3+} from the chelate complex with increased tissue retention time. Presumably, the concept demonstrated in this study may be applied to the design of other macromolecule-based MRI contrast agents. Using a protein to chelate Gd^{3+} as an MRI contrast agent has several potential advantages over Gd^{3+}−DTPA in functional and molecular imaging applications: (1) it greatly increases the CNR; (2) it improves dose efficiency with reduced metal toxicity; (3) it prolongs the tissue retention time, which enables imaging of an abnormality that requires prolonged tissue enhancement; and (4) it provides a potential functioning protein or a protein carrier that can conjugate target-specific ligands to a biomarker for targeted molecular MR imaging. Despite the fact that the diffusion rate of protein with proper size (3−5 nm) is slower than that of small chelators, limiting its capability to diffuse to the target, we expect to develop and investigate biomarker targeted molecular imaging in the immediate future with our protein-based contrast agents since the affinity and specificity of molecular recognition is largely dependent upon the proper balance between the on and off rates. Although immunogenicity is a concern when using a protein as a matrix of Gd^{3+} carrier, we expect that such limitations may be overcome by improved design of protein carrier and the success of protein drugs.[60]

Supporting Information Available: ESI-MS of metal/protein complex, determination of metal binding constants, MRI imaging and its data analysis, tissue retention and blood circulation time of contrast agents, toxicity, and simulation of contrast agent relaxivities. This material is available free of charge via the Internet at http://pubs.acs.org.

JA800736H

(54) van Zijl, P. C.; Jones, C. K.; Ren, J.; Malloy, C. R.; Sherry, A. D. *Proc. Natl. Acad. Sci. U.S.A.* **2007**, *104* (11), 4359–4364.

(55) Lauffer, R. B.; Parmelee, D. J.; Ouellet, H. S.; Dolan, R. P.; Sajiki, H.; Scott, D. M.; Bernard, P. J.; Buchanan, E. M.; Ong, K. Y.; Tyeklar, Z.; Midelfort, K. S.; McMurry, T. J.; Walovitch, R. C. *Acad. Radiol.* **1996**, *3*, S356–358.

(56) Lauffer, R. B.; Parmelee, D. J.; Dunham, S. U.; Ouellet, H. S.; Dolan, R. P.; Witte, S.; McMurry, T. J.; Walovitch, R. C. *Radiology* **1998**, *207* (2), 529–538.

(57) Parmelee, D. J.; Walovitch, R. C.; Ouellet, H. S.; Lauffer, R. B. *Invest. Radiol.* **1997**, *32* (12), 741–747.

(58) Allen, M. J.; Meade, T. J. *J. Biol. Inorg. Chem.* **2003**, *8* (7), 746–750.

(59) Brasch, R.; Turetschek, K. *Eur. J. Radiol.* **2000**, *34* (3), 148–155.

(60) Stockwin, L. H.; Holmes, S. *Expert Opin. Biol. Ther.* **2003**, *3* (7), 1133–1152.